Results in Engineering 25 (2025) 103614

Contents lists available at ScienceDirect

Results in Engineering

journal homepage: www.sciencedirect.com/journal/results-in-engineering

Design of sub-6 GHz BPF using chained even and odd mode admittance polynomials for 5G C-band applications

Francis Emmanuel Chinda [a,c], Mehwish Hanif [b,*], Socheatra Soeung [c], Muhammad Sani Yahya [c,d], Ahmed Jamal Abdullah Al-Gburi [e,*], Faisal Bashir [f], Furqan Zahoor [f], Cheab Sovuthy [g]

[a] Department of Computer Engineering Federal University Wukari Taraba State, Nigeria
[b] Tyndall National Institute, University College Cork, Lee Maltings, Cork, T12 R5CP, Cork, Ireland
[c] Dept. of Electrical and Electronic Engineering Universiti Teknologi Petronas, Sri Iskandar,Perak, Malaysia
[d] Department of Electrical and Electronic Engineering, Abubakar Tafawa Balewa University Bauchi, Nigeria
[e] Center for Telecommunication Research & Innovation (CeTRI), Fakulti Teknologi dan Kejuruteraan Elektronik dan Komputer (FTKEK), Universiti Teknikal Malaysia Melaka (UTeM), Melaka 76100, Malaysia
[f] Department of Computer Engineering, College of Computer Science and Information Technology, King Faisal University, Al-Ahsa 31982, Saudi Arabia
[g] School of Digital Engineering, Cambodia Academy of Dig. Technology, Phnom Penh, Cambodia

ARTICLE INFO

Keywords:
Bandpass filter (BPF)
Compact filters
5G applications
Chained filtering functions
Chebyshev
Selectivity
Stability

ABSTRACT

This paper presents the design of a Bandpass filter (BPF) using chained even and odd mode admittance polynomials for 5G sub-6 GHz C-band applications. The filter will offer a reduced sensitivity to fabrication tolerance and still maintain its response in comparison to traditional Chebyshev filters. A new transfer function based on chained filtering functions (CFFs) for fourth-order filters is derived in even and odd mode admittances and the synthesis methods are presented. To demonstrate the feasibility of the proposed approach, a 4^{th}-order chained-function filter (CFF) operating at the center frequency of 3.5GHz with a bandwidth of 40MHz is designed, synthesized, and fabricated. The circuit simulation is carried out in advanced simulation software (ADS). The filter prototype is fabricated in parallel-connected topology using an open-loop microstrip resonator, the size of the filter is 2.5cm x 4cm. The simulation and measured insertion/return loss are 0.40dB / 20dB and 2.5dB/ 18.08dB, and the achieved selectivity is 87.5. Considerable Sensitivity analysis to prove the filter fabrication tolerance is conducted and its reliability is proven by theoretical analysis. The prototype result in this work is validated and agrees well with the theoretical results. In terms of practical implementation, this design technique will serve as a very useful mathematical tool for filter design engineers.

1. Introduction

Manufacturers are under constant pressure to reduce the time and cost of developing microwave hardware devices for 5G applications [1,2]. Designing a filter with high performance requires superior materials, precise assembly, and post-production tuning. Significant efforts have been made resulting in enhanced electromagnetic (EM) simulation tools to design such filters [3,4]. The challenges have been shifted to manufacturing processes due to improvements in simulation tools. Therefore, to completely leverage and benefit from the enhanced modeling of precision, the hardware must now be designed and manufactured with a very low tolerance level [5,6]. Currently, most of the millimeter and microwave BPF being developed and produced are made up of the traditional Chebyshev class [7,8]. This family of filters has a specific order and gives the best rejection for an equiripple response. The frequency distribution of return-loss (RL) zeros is one of the critical factors in obtaining a good filter response [9,10]. The relative frequency separation of RL zeros for higher-order filters becomes extremely small, which requires high accuracy in the manufacturing process. Post-manufacturing turning technique is required to reconfigure the filter response back to its original response [11,12]. To solve this problem, the constraint of the existing production technologies and the filter sensitivity to fabrication processes must be addressed at the design preliminary stage of the approximation [13]. To achieve this, the

* Corresponding authors.
E-mail addresses: Mehwishhanif1991@gmail.com (M. Hanif), ahmedjamal@ieee.org (A.J.A. Al-Gburi).

https://doi.org/10.1016/j.rineng.2024.103614
Received 16 August 2024; Received in revised form 19 November 2024; Accepted 2 December 2024
Available online 10 December 2024

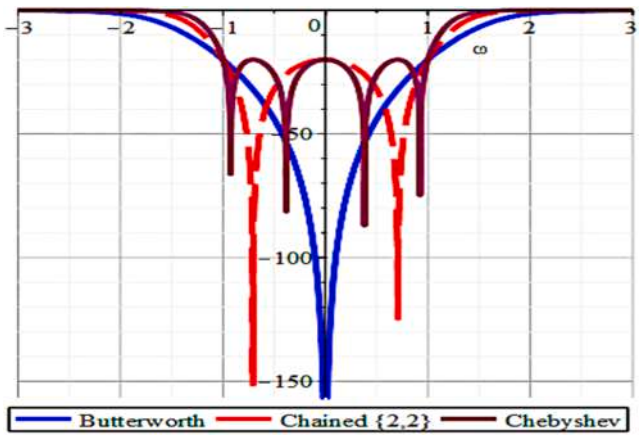

Fig. 1. CF characteristics compared to Butterworth and Chebyshev filters response.

Table 1
Theoretical separation distance of return loss frequencies for n = 5.

$n_{s(k)}$	$\delta\omega_{min}$
2	1.4142
3	0.8660
4	0.5412
5	0.3633

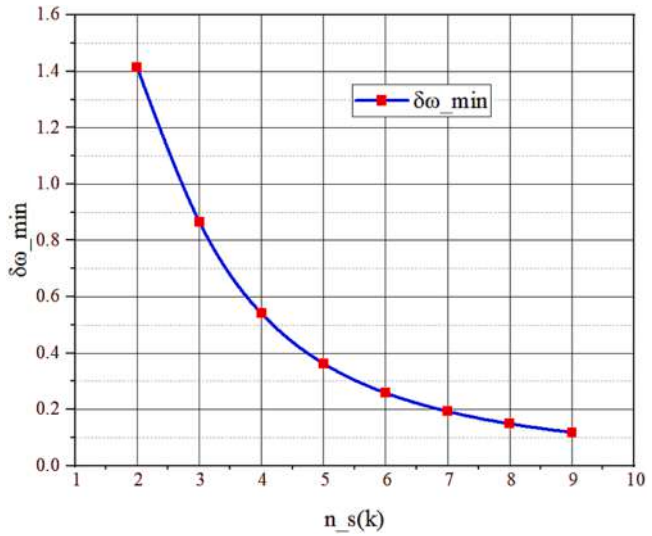

Fig. 2. Theoretical plot to demonstrate the frequency separation distance of chained RL.

required filter specifications are simulated using a transfer function that is of higher order and reduced sensitivity. The new class of filtering function known as chained is formed by multiplying the low-order function of traditional Chebyshev polynomials [14,15]. The chained filtering function polynomials can be found as a compromise between Butterworth and Chebyshev approximations [6,16]. The technique provides different transfer functions to choose from, each with unique characteristics and implementation requirements. The chained transfer functions can reduce filter design complexity, fabrication tolerance, and post-manufacturing tuning processes [17,18]. Hence, they have the potential to extend the current state-of-the-art production of higher-performance tuning-less filters to higher operating frequencies and narrow bandwidth implementations [8,19].

This paper presents a new technique to design, synthesize, and implement the chained function filter using even and odd mode admittances for 5G sub-6GHz C-band applications. To prove the feasibility of this technique, a fourth-order filter prototype is fabricated and measured results are included.

This paper is structured as follows. Section 2 presents a clear theory and chained filtering function characteristics. Section 3 presents the filter synthesis procedure and results respectively. Section 4 presents the circuit simulation and results Section 5 presents the filter physical layout design. Sections 6 and 7 discussed the filter prototype, measured results, and sensitivity analysis results, and finally, Section 8 concluded. The main contributions of this paper are as follows:

a) This work introduced a new filtering function called chained for even and odd mode admittance, that can effectively place multiple RL zeros at the same frequency. The function can be used to design both symmetrical and asymmetrical filters across a broad range of frequencies and technologies. The filtering function offers the advantage of producing compact filters with reduced sensitivity to fabrication tolerance for 5G sub-6GHz C-bands. This polynomial will serve as a valuable mathematical tool for filter design engineers to improve performance and simplify design.
b) This work introduced a technique to realize a CFF prototype using open-loop microstrip resonators in parallel-connected structures. This will further improve the filter tuning processes for faster production at low- cost. The enhanced tolerance properties and compact size of the filter make it a potential candidate for integration into front-end subsystems and deployment in 5G sub-6GHz C-bands applications.

2. The chained filtering functions characteristics

The characteristics of the chained filtering function polynomial are presented in Fig. 1. The figure demonstrates that the passband ripple of the chained function (CF) is a compromise between the ripples of Butterworth and Chebyshev polynomials [20,21]. The Chained ripples tend to overlap and form two poles spaced apart [22,23]. The Chebyshev model is the closely spaced four-pole equiripple response, which necessitates higher manufacturing tolerance while the Butterworth response has only one pole in the passband. The chained CFF can be determined by properly choosing the suitable seed function in the order of {2,2} combination [18]. The filter selectivity will result in less sensitivity to manufacturing error in comparison to the Chebyshev counterpart [24]. Its rejection performance is better than Butterworth's but slightly less than Chebyshev's. This filter family is not only limited to reducing its sensitivity but will lead to enhanced design complexity [20].

2.1. The chained filtering function return-loss zeros characteristics

The CFF reflection zeros are not evenly spaced in the passband. The zeros closest to the cut-off frequency will have the smallest separation distance [25,4,26]. Thus, the separation distance for chained RL can be determined using Eq. (1).

Table 2
The seed function combination for fourth order chained function.

No. of Seed Function	Seed-Function Order	Polynomial Function
4	{1,1,1,1}	ω^4
3	{1,1,2}	$2\omega^4$- ω^2
2	{2,2}	$4\omega^4$- $4\omega^2$ +1
2	{3,1}	$4\omega^4$- $3\omega^2$
1	{4}	$8\omega^4$- $8\omega^2$ +1

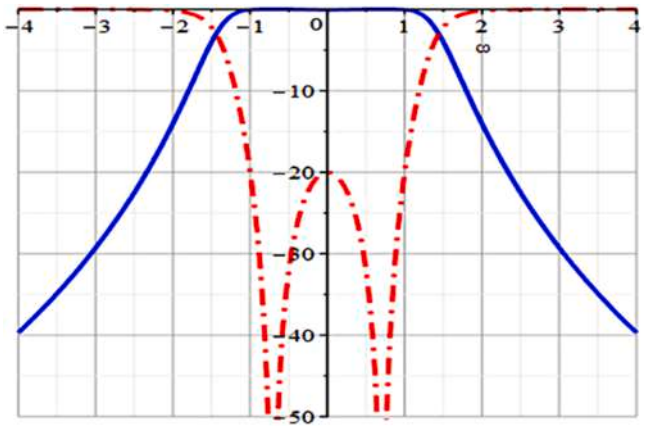

Fig. 3. The fourth-order CF theoretical plot.

$$\delta\omega_{\min} = 2\sin\left(\frac{\pi}{n_{s(k)}}\right)\sin\left(\frac{\pi}{2n_{s(k)}}\right) \tag{1}$$

$\delta\omega_{min}$ Represent minimum frequency distribution distance while $n_{s(K)}$ represents the filter order.

To demonstrate the feasibility of this equation, the values of (ns(k)) are chosen from 1 to 5. The outcome proves that the highest possible separation distance for CFF can be achieved from N =2. Thus, by increasing the filter order (N) the frequency separation distance of return loss decreases [27,28]. This approach can effectively position multiple RL for CFF at the same frequencies, thereby enhancing its fabrication processes and reducing sensitivity. Table 1 displays the chained minimum separation distance values obtained to prove Eq. (1) while Fig. 2 illustrates the theoretical plot.

2.2. Seed filtering function formation

The CFF is formed by multiplying the lower-order product of the traditional Chebyshev polynomial called seed function [29,30]. Table 2 presents the fourth-order chained combinations formed from lower-order seed function polynomials of conventional Chebyshev [31]. In the Table, the first row represents the approximation of Butterworth polynomials while the last row represents the approximation polynomials for conventional Chebyshev of the same order [32].

2.3. The selection of seed function polynomial

The transfer and reflection functions response are theoretically plotted for all possible seed functions combinations for the fourth-order filter to predict its optimum performance within the passband in terms of transmission and reflection powers while maintaining an RL of 20 dB and a specific ripple factor (ε) of 0.1005 [33]. Based on the expected results, the seed function polynomial in Eq. (2) is selected for the synthesis of fourth order filter [34]. This response provides the expected behaviors of the filtering under ideal situations and based on the response, the polynomial in (2) is chosen for the synthesis of the filter. Fig. 3 presents the theoretical plot for fourth fourth-order chained function filter.

Table 3
The forth-order LP circuit parameters.

Components	Low-Pass Values
$C_1 = C_2$	1.09F
$C_3 = C_4$	2.16F
$J_{S1} = J_{2L}$	1
$J_{S3} = J_{4L}$	1
J_{12}	0.83
J_{34}	-3.3023

$$F_N = 4\omega^4 - 4\omega^2 + 1 \tag{2}$$

3. The filtering function synthesis technique

The synthesis technique for the parallel chained function filter is based on the use of even and odd-mode admittance expression of a low-pass (LP) prototype network [9]. These expressions are divided into sub-networks connected from source (P1) to load (P2). The sub-branches exhibit similar characteristics as ladder networks when combined [35]. The network can be synthesized by solving the functions F_U, S_{11}, and S_{21} in Fig. 4. Illustrate the LP inverter coupled network for chained function.

$$F_U = \frac{j}{2}\left(\prod_{r=1}^{N}\left\{\frac{1+kk_r+\left[\left(1+k^2\right)\left(1+k_r^2\right)\right]^{\frac{1}{2}}}{k-k_r}\right\}\right) + \prod_{r=1}^{N}\left\{\frac{1+kk_r-\left[\left(1+k^2\right)\left(1+k_r^2\right)\right]^{\frac{1}{2}}}{k-k_r}\right\} \tag{3}$$

$$|S_{11}(\omega)|^2 = \frac{\varepsilon^2 F_U^2(\omega)}{1+\varepsilon^2 F_U^2(\omega)} \tag{4}$$

$$|S_{21}(\omega)|^2 = \frac{1}{1+\varepsilon^2 F_U^2(\omega)} \tag{5}$$

Where U represents the filter order, k, j, and k_r are the locations of transmission zeros (TZ), The Y_e (even-mode) and Y_o (odd-mode) admittances polynomials can be derived by solving the roots of function $S_{11}(k)$ as described in [36], while the ABCD transfer function matrix can be formed using appropriate expressions described in [37], and by employing partial fraction expansion will results in placement of the resonators into parallel network [38].

$$S_{21}(p) = \frac{Y_e - Y_o}{(1+Y_e)(1+Y_o)} \tag{6}$$

$$S_{11}(p) = \frac{(1-Y_eY_o)}{(1+Y_e)(1+Y_o)} \tag{7}$$

3.1. Synthesis of fourth-order CF filter using even and odd mode J-admittances

The complete synthesis technique of the fourth-order CFF using even and odd-mode J-admittances is presented. The filtering function is formed by chaining the polynomial of the Chebyshev seed function of the first kind [11]. The synthesis technique involves deriving the even

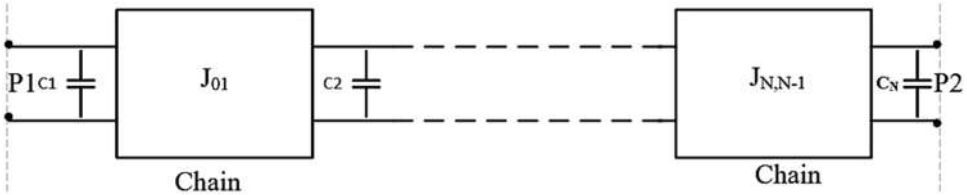

Fig. 4. LP inverter coupled chained function network.

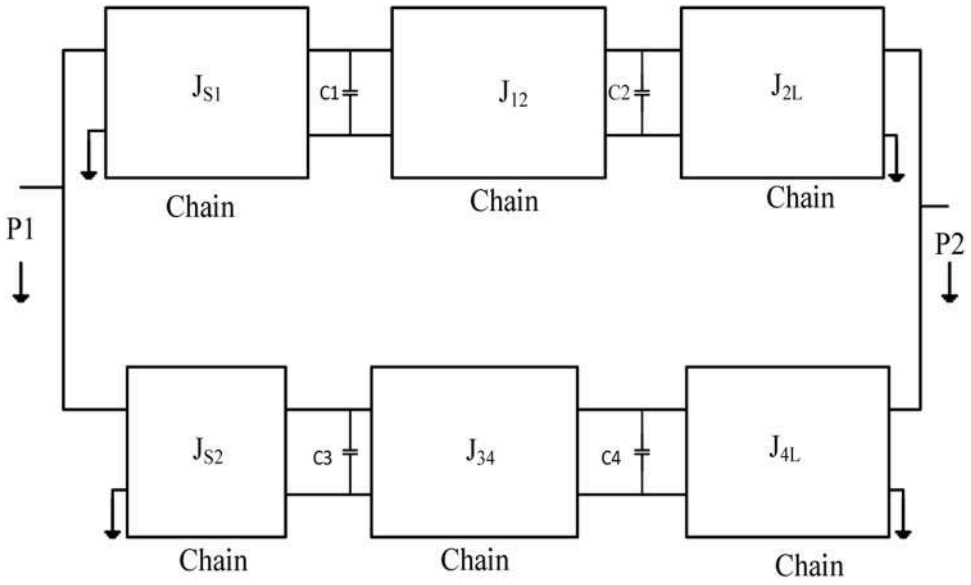

Fig. 5. Fourth-order LP circuit layout.

and odd mode admittances of the filter from Eq. (1). The synthesis steps are as follows:

First Step: The zeros can be derived from the S-parameters as presented in equation (8)

$$k^8 + 2k^6 + 1.5k^4 + 0.5k^2 + 6.25 = 0 \tag{8}$$

Second Step: The polynomials in the left-hand plane are defined by equations (9) and (10)

$$k = -0.4168935436 \pm j1.337545733 \tag{9}$$

$$k = -0.9718282536 \pm j0.5737785234 \tag{10}$$

Third Step: The transfer function of the chained filtering can be obtained by representing the network as two- -parallel branches is first determined, and the roots of S_{11} and S_{11} are used to formulate the polynomial P(p), as presented in Eq. (11).

$$k(k) = k^2 + 1.388721797k + j0.7637672 + 1.172603940 - j1.060660172 \tag{11}$$

Fourth Step: The zeros of P(p) are identical to the zeros of 1+Ye(p) and can be calculated using the expression in Eq. (12)

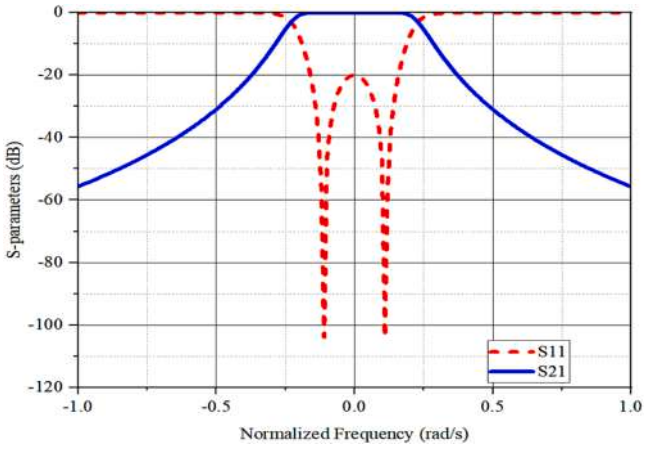

Fig. 6. Fourth-order LP S-parameter response.

$$1 + Y_e = 1 + \frac{N(k)}{D(k)} \tag{12}$$

Fifth Step: The polynomials for complex even and odd modes are derived from Eqs. (8) to (15).

$$N(k) = k^8 - j0.7638k + 1.1726 \tag{13}$$

$$D(k) = 1.3887k - j1.06066 \tag{14}$$

By using equation (13)

$$Y_e(k) = \frac{N(k)}{D(k)} = \frac{k^2 - j0.7638k + 1.17260}{1.3887k + j1.06066} \tag{15}$$

Sixth Step: By applying Eq. (15), a unity even-mode admittance inverter can be inserted before the network, allowing Ye to be expressed as.

$$Y'_e(k) = \frac{1.3887k - j1.06066}{k^2 + j0.7638k + 1.17260} \tag{16}$$

Seventh Step: The denominator can be decomposed into simpler components using partial fraction expansion, and Ye can be divided into two distinct parts, as described in reference [57].

$$Y'_e(k) = \frac{1}{1.0807k + j0.8282} + \frac{1}{2.1578k - j3.3017} \tag{17}$$

$$Y'_o(k) = \frac{1}{1.0807k - j0.8282} + \frac{1}{2.1578k + j3.3017} \tag{18}$$

Eight Steps: This approach can be similarly applied to the odd-mode admittance network, yielding identical outcomes.

Ye and Y_o can be further split into four parallel branches by dividing Eqs. (17) and (18) by 2.

Table 4
Fourth-order chained BPF circuit parameters.

Parameters	Band-Pass Values
$L_1 = L_2$	0.002nH
$L_3 = L_4$	1.015nH
$C_1 = C_2$	991.4pF
$C_3 = C_4$	748.4pF
J_{12}	0.828
J_{34}	-3.302

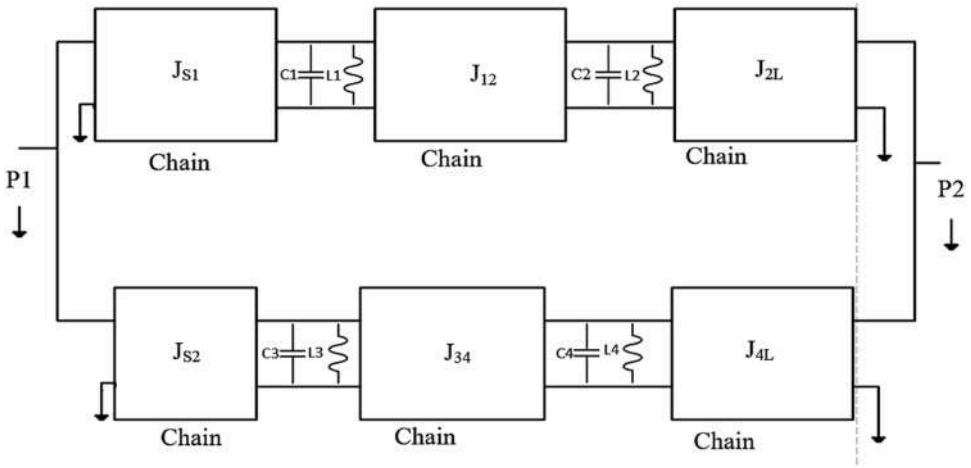

Fig. 7. Fourth-order chained BPF layout.

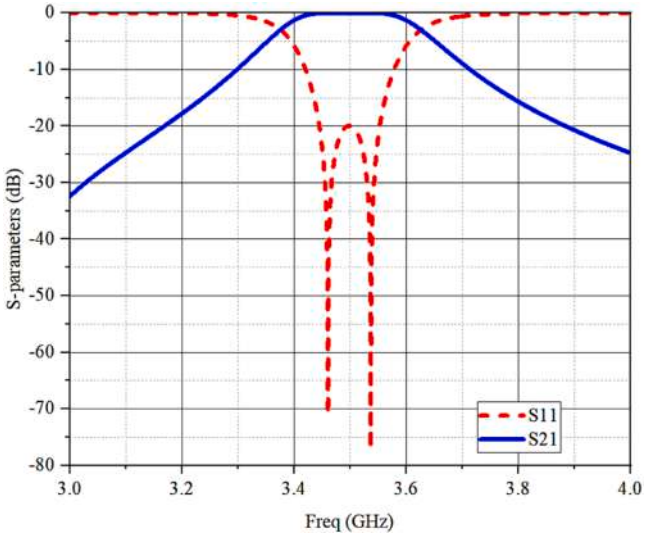

Fig. 8. Fourth-order chained BPF S-parameter response.

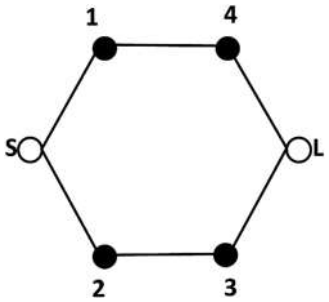

Fig. 9. Fourth-order chain filter routing structure.

Table 5
The filter design parameter.

Parameters	Specifications
Filter order *(n)*	4
Center frequency *(f_o)*	3.5GHz
Bandwidth *(BW)*	$\geq$ 40 MHz
Return Loss *(RL)*	20
Insertion Loss *(IL)*	$\leq$ 3 dB

Table 6
The coupling coefficient (K) versus distance (S).

S(mm)	f_1 (GHz)	f_2 (GHz)	*K*
0.5	3.45	3.62	0.0067
1.0	3.51	3.59	0.0345
1.5	3.53	3.58	0.0176
2.0	3.55	3.56	0.0059

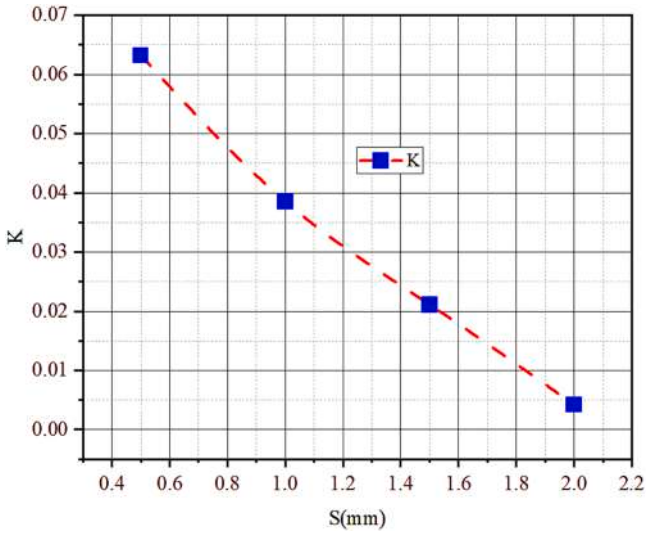

Fig. 10. The filter (K) versus (S) characteristics.

$$Y_e'(k) = \frac{2}{2(1.0807k - j0.8282)} + \frac{2}{2(2.1578k + j3.3017)} \tag{19}$$

$$Y_o'(k) = \frac{2}{2(1.0807k + j0.8282)} + \frac{2}{2(2.1578k - j3.3017)} \tag{20}$$

The numerator values formed J-admittance, while the denominator form the capacitance values. The potential advantage of this technique is that it gives flexibility in the choice of multiple parallel branches as it allows filter designers to freely place resonators in the network. This technique can be applied in the design of higher-order odd-mode symmetrical filter networks.

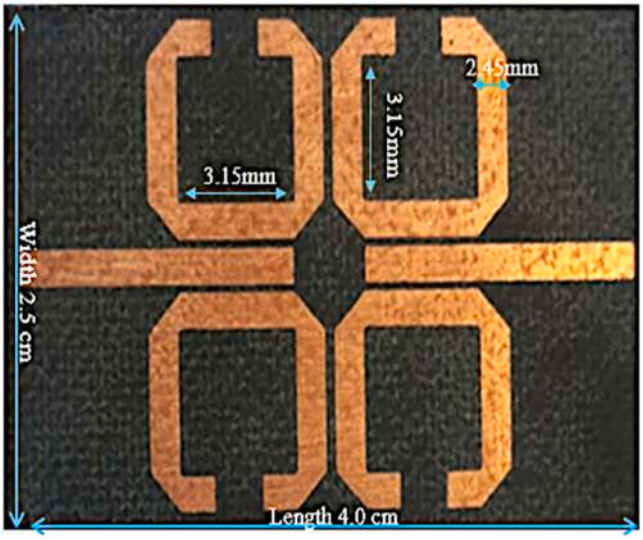

Fig. 11. The fourth-order CFF physical layout.

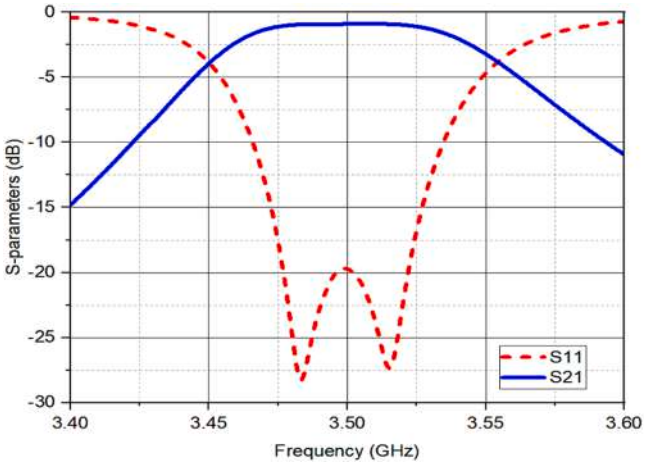

Fig. 12. Fourth-order CFF simulation response.

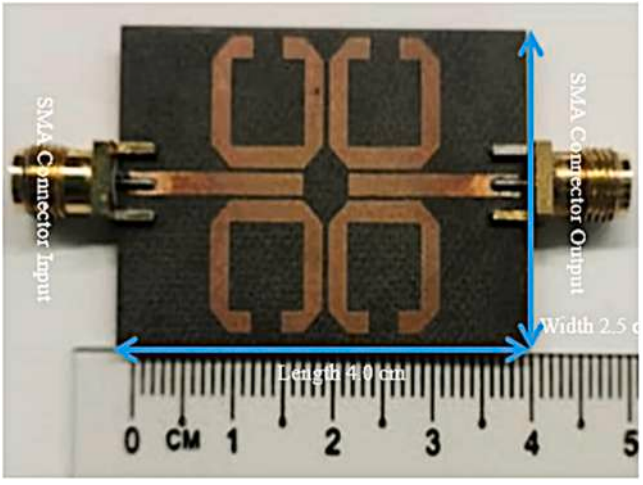

Fig. 13. The microstrip prototype of CFF.

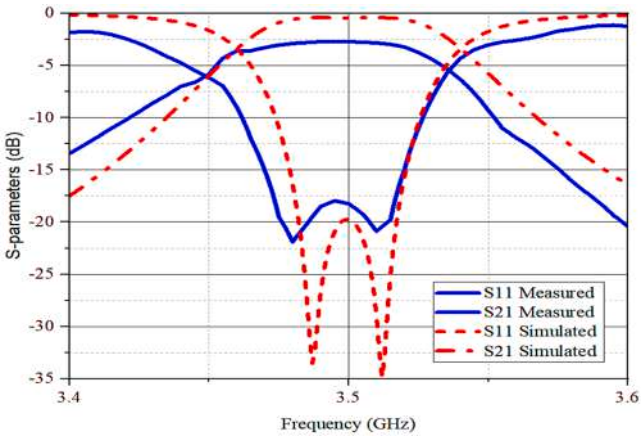

Fig. 14. The simulated and measured responses of CFF.

Table 7
Summary of impacts on 4th order Cff.

S/No	4th Order CFF Applied Tolerance	RL Change (%)
1	-0.5%	1.09%
2	+5%	2.14%
3	-1%	1.12%
4	+1%	2.18%
5	-2%	1.14%
6	+2%	2.22%

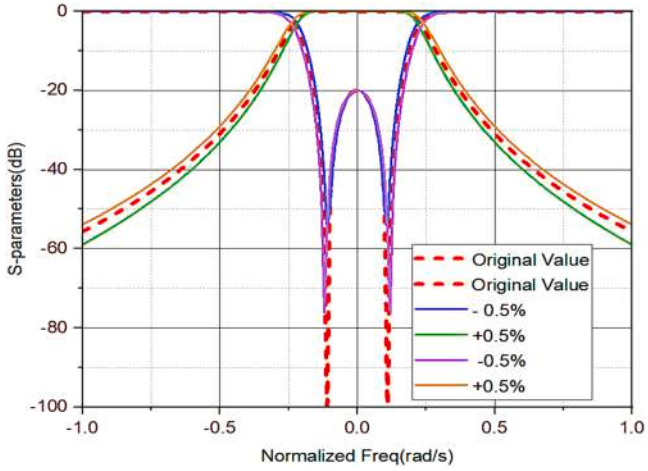

Fig. 15. ± 0.5% Tolerance impacts on the filter.

4. The circuit simulation of chained function filter

The J-admittance and capacitance values obtained in Eq. (17) are transformed into a schematic low-pass parallel network for the fourth-order chained filter to assess its low-pass performance. The simulation is carried out in advanced simulation software (ADS). Table 3 provides an overview of the low-pass parameters of the network. The schematic low-pass network is presented in Fig. 5, while Fig. 6 shows the S-parameter response.

This technique can serve as a guide to simulate any two-port even and odd mode chained filter networks sub-divided into branches and connected in parallel from source (S) to Load (L). This network. This will

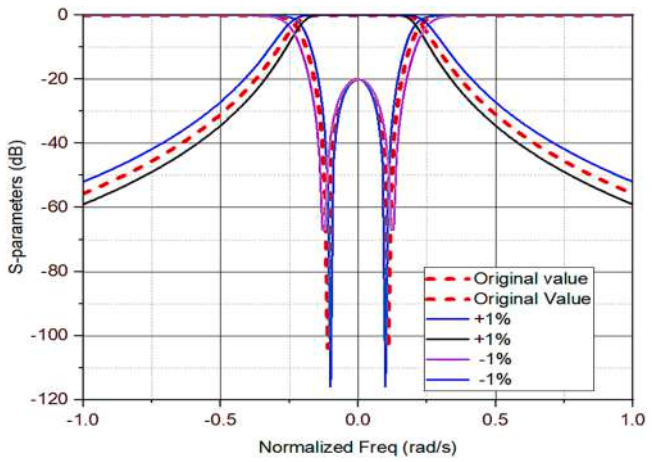

Fig. 16. ± 1% Tolerance impacts on the filter.

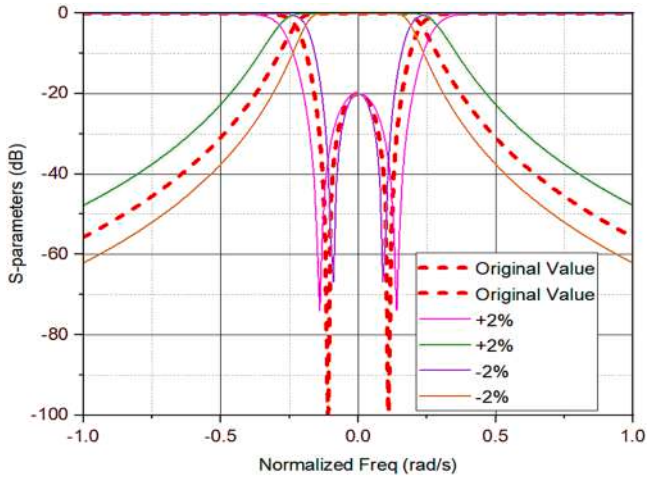

Fig. 17. ± 2% Tolerance impacts on the filter.

provide the same properties as ladder networks when combined [39]. Filters with a specified order can have similar configurations regardless of the number of transmission zeros used in the transfer function [30]. This will serve as a useful tool in synthesizing multiple parallel branch filter networks simultaneously.

4.1. The chained function BP transformation

The low-pass (LP) parameters of the filter are converted into a BPF by using the suitable capacitive transformation equations in equations [13] and [40] to determine its performance in BP networks. The inductance and capacitance parameters of the BPF are summarized in Table 4. Fig. 7, presents the BPF schematic layout while Fig. 8 shows its S-parameter response.

The Fourth-order chained BPF network has generated two poles at the center frequency of 3.5 GHz and an RL of 20dB as expected. This confirms narrowband and excellent response in terms of signal reflection. The spacing of RL frequencies further apart confirms that the filter is less sensitive to fabrication variations that may occur during the manufacturing processes. The response aligns with the theoretical one, demonstrating consistency between the actual result and the expected outcomes.

4.2. The filter coupling matrix extraction

The procedure to obtain the coupling matrix of the filter involves mapping and extracting it from the derived filtering function by using the appropriate equations in [21,41]. The transmission and reflection coefficients S_{11} and S_{21} are used to derive the filter coupling matrix of the network [42]. A reduction method is used to derive the coupling matrix structure in which the row of the matrix is achieved [43]. Similarity transformation and matrix element annihilation are carried out to obtain the overall coupling matrix, *M*, as described in [44,14]. The synthesized coupling matrix is then sub-divided into networks and a series of configurations are performed for the entire matrix until suitable coupling is achieved. The complete coupling matrix, M for the fourth-order chained filter is presented in Eq. (21) which translates to N+2 configurations and routing topology is shown in Fig. 9. Letters S and L represent the input and the output of the filter while numbers from 1 to 4 correspond to resonator positions.

$$M = \begin{pmatrix} 0 & 0.68 & 0.96 & 0 & 0 & 0 \\ 0.68 & 0 & 0 & 0 & 1.53 & 0 \\ 0.96 & 0 & 0 & 0.77 & 0 & 0 \\ 0 & 0 & 0.77 & 0 & 0 & -0.96 \\ 0 & 1.53 & 0 & 0 & 0 & 0.68 \\ 0 & 0 & 0 & -0.96 & 0.68 & 0 \end{pmatrix} \tag{21}$$

5. Chained BPF design and simulation procedures

This section presents the general overview of CFF realization. The synthesized network can be realized on a microstrip resonator if the Q-factor is 300 or lower [21,22]. The filter's initial design parameters are presented in Table V. An open loop microstrip resonator is selected for this work due to its simplicity in tuning and inherent properties of reduced sensitivity [14]. The ideal circuit is converted into a microstrip physical layout by specifying the length (L) and width (W) of the resonators alongside the loss and the other specifications defining the microstrip properties. At this stage, an excellent coupling between the resonators is achieved by extracting the external quality factor (Qe) and filter coupling coefficient (K) [45]. The initial filter design specifications are presented in Table 5.

Table 8
Comparison of the design filter with related publications.

Study	f_o (GHz)	Filter order	ε_r	*h* (*μm*)	IL [2] (dB)	IL [3] (dB)	Selectivity [3]
[9]	2.45	4	9.5	635	1.7	13	83
[14]	2.2	5	10.8	1.27	0.9	19.2	5
[20]	2.4	4	2.2	787	1	15	8.3
[23]	0.96	6	2.2	787	4	16	24
[31]	2.65	5	3.38	580	2	12.6	8.4
[32]	0.9	6	3.6	508	2.8	14	60
[33]	2.4	4	2.55	800	5.2	10	68
[49]	3.98	3	3.55	0.813	10.52	0.86	7.24
[50]	6.55	3	1.524	0.813	22.5	1.15	3.7
This Work	3.5	4	2.2	787	2.5	18.08	87.5

5.1. The filter inter-resonators coupling

The inter-resonator coupling can be achieved by adjusting the distance or gap between the resonators. The coupling setup between the adjacent resonators is mixed-coupling [24]. The values of (K) in Table VI are obtained using the line calculations technique in ADS and Eq. (22). Inter-resonator coupling can be achieved by carefully adjusting the gap or distance between the resonators and recording the resonant frequencies. Table 6 presents the coupling coefficient values of the resonators, while Fig. 10 shows the plot of coupling coefficients (K) versus the gap (S) between the resonators. The (K) decreases as the distance or gap (S) increases and vice versa. This implies, that smaller coupling coefficients mean weaker resonator coupling.

$$K = \frac{f_0}{BW} \times \frac{f_2^2 - f_1^2}{f_2^2 + f_1^2} \tag{22}$$

Where f_o represents the center frequency, BW is the filter bandwidth, while f_1 and f_2 are the frequencies of the first and second eigenmodes and K is the coupling factor.

5.2. The filter physical layout design

The proposed CFF layout is developed using open-loop microstrip resonators connected in parallel following the structure in Fig. 9. The filter layout simulation is conducted on advanced design simulation (ADS) software with the filter layout and simulation performances presented in Figs. 11 and 12. The filter layout design has produced 2-poles as expected for the chained function at the center frequency of 3.5GHz. The achieved simulation return loss is better than 20dB with a minimum insertion loss of 0.4 dB. The layout BW and FBW are 46.79MHz and 1.33%. These findings have been validated and are in good agreement with the theoretical performance. This outcome demonstrates the main advantage of the CF polynomial which efficiently positions multiple return loss zeros at the same frequency, Thus, resulting in producing filters with reduced sensitivity to manufacturing tolerance while still preserving its response within the specified passband. Theoretically, the filter has proven to offer good rejection levels compared to Chebyshev filters provided the appropriate seed functions are selected.

6. The filter prototype and results

The prototype of the filter is fabricated on RT/Roger duroid 5880 microstrip substrate, with a thickness of 787 μm and a copper-clad thickness of 17.5 μm, the dielectric constant (εr) of 2.2, a loss tangent (tan δ) of 0.0009, and an electrical length of 180° which is $\lambda/2$ are used [46]. The dimensions of the resonator's width and length are 2.45 mm and 3.15 mm. The input/output ports of the filter are connected to 3.5 mm SMA connectors. The feed lines between the resonators are 10mm. The filter's overall circuit size is 2.5cm x 4cm. The prototype of the filter is shown in Fig. 13, while the simulation and measured performances are presented in Fig. 14. The ability of the filter to produce two poles within the desired bandwidth at the center frequency of 3.5GHz is achieved and proven. The simulated and measured values of IL/RL achieved are 0.4dB/20dB and 2.5dB/18.08 dB, a BW of 40MHz and FBW of 1.14%. A shift of 0.217% is observed in the measured bandwidth. The shift is a result of calibration cable loss, discontinuities in the microstrip line junctions, package parasitic effects, dielectric loss effects of the material, SMA soldering port, and ground effects. The filter transmission zeros (TZs) can be controlled by changing the values of source capacitors and the load coupling. This result agrees well with the theoretical analysis. The shift in the measured bandwidth should be considered for a specific application.

7. Sensitivity analysis

Sensitivity analysis is performed on the CFFs to prove that the filter can be fabricated with better tolerance and still preserve its response in specified bandwidth compared to traditional Chebyshev counterparts [47,48]. To validate the effects of manufacturing tolerance on the filter, various experiments are conducted in which the initial component values are modified to have a difference of ± 0.5%, ± 1%, and ± 2%. The distribution variance was selected according to the filter fabrication machine's specified maximum tolerance of approximation. Table 7 summarizes the tolerance parameters of the filter while Figs. 15-17 presents the S-parameter performance of the filter when tolerance is applied. These results prove that CFFs connected in parallel are less sensitive to fabrication tolerance and preserve selectivity compared to Chebyshev filters. This is demonstrated by the reduced percentage shift in return loss when random error is applied. The wider spacing of filter poles confirms improved manufacturing tolerance.

8. Comparison with related work

Table 8 compares the realized filter in this work with related research. This filter has demonstrated a significant improvement in terms of insertion loss (IL), return loss (RL), and size compared to the previous work considering the filtering function and topology setup. The compact size and enhanced selectivity of our filter make it a promising candidate for integration into 5G sub-6GHz C-bands applications.

9. Conclusion

A Fourth-order prototype of a chained function filter in a parallel structure was designed and fabricated. The overall circuit size of the filter is 2.5cm x 4cm. The achieved measured IL/RL is 2.5 dB/18.08 dB while the selectivity is 87.5. The theoretical and measured results were validated and in good agreement with each other. Extensive sensitivity analysis was performed and the results have proven the fabrication tolerance of the filter. The advantage of this filter prototype is that it offers reduced sensitivity to fabrication tolerance and still preserves its response within a specific bandwidth comparable to Chebyshev filters. The filter-reduced sensitivity to fabrication error is fully demonstrated using open-loop microstrip technology and its reliability is proven. The implementation of this filter is not limited to microstrip technology and parallel structure but can be applied to any given technology and topology available. Lower and higher-order filters can easily be implemented using CFF polynomial, thereby serving as a very beneficial mathematical tool for filter design engineers.

CRediT authorship contribution statement

Francis Emmanuel Chinda: Writing – original draft, Software, Methodology, Investigation, Formal analysis. **Mehwish Hanif:** Writing – review & editing, Resources, Project administration, Funding acquisition, Conceptualization. **Socheatra Soeung:** Visualization, Supervision, Methodology. **Muhammad Sani Yahya:** Methodology, Formal analysis. **Ahmed Jamal Abdullah Al-Gburi:** Software, Methodology, Formal analysis. **Faisal Bashir:** Writing – review & editing, Validation, Project administration. **Furqan Zahoor:** Writing – review & editing, Validation, Formal analysis, Data curation. **Cheab Sovuthy:** Visualization, Formal analysis, Data curation.

Declaration of competing interest

The authors declare that they have no known competing financial interests or personal relationships that could have appeared to influence the work reported in this paper.

Acknowledgment

This study was supported by the University College Cork. The authors would also like to thank the Department of Electrical and Electronic Engineering as well as the Centre of Graduate Studies (CGS) in Universiti Teknologi PETRONAS (UTP) for providing the research facilities.

Data availability

No data was used for the research described in the article.

References

[1] S.I. Yahya, F. Zubir, L. Nouri, N.M. Jizat, An ultra-compact microstrip bandpass filtering coupler with suppressed harmonics and low group delay: A novel structure for 5G applications, Results. Eng. 24 (Dec. 2024), https://doi.org/10.1016/j.rineng.2024.103003.

[2] M.A.E. Eid, T.G. Abouelnaga, H.A. Ibrahim, E.K.I. Hamad, A.J.A. Al-Gburi, T.A. H. Alghamdi, M. Alathbah, Highly Efficient GaN Doherty Power Amplifier for N78 Sub-6 GHz Band 5G Applications, Electronics. (Basel) 12 (2023) 4001, https://doi.org/10.3390/electronics12194001.

[3] Y. Khardioui, A. El Alami, M. El Ghzaoui, Design and optimization of a compact microstrip BPF for wireless communication systems based on open-loop rectangular resonators, Results. Eng. 21 (Mar. 2024), https://doi.org/10.1016/j.rineng.2024.101941.

[4] R.H. Elabd, A.J.A.A. Gburi, J. Alsayaydeh, An ultra-selective OLR-based microstrip diplexer with minimal insertion loss for wireless communication system, Int. J. Intell. Eng. Syst. 17 (2) (2024) 83–94.

[5] Z. Zhang, et al., Microwave Displacement Sensors Based on Filtering Phase Shifter with Chebyshev Response, IEEE Sens. J. 24 (10) (May 2024) 15857–15864, https://doi.org/10.1109/JSEN.2024.3379754.

[6] O. Diouri, A. Gaga, H. Ouanan, S. Senhaji, S. Faquir, M.O. Jamil, Comparison study of hardware architectures performance between FPGA and DSP processors for implementing digital signal processing algorithms: Application of FIR digital filter, Results. Eng. 16 (Dec. 2022), https://doi.org/10.1016/j.rineng.2022.100639.

[7] G. Chaudhary, Y. Jeong, A Tunable Bandpass Filter with Arbitrarily Terminated Port Impedance Using Dual-Mode Resonator, J. Electromagnet. Eng. Sci. 22 (6) (2022) 647–655, https://doi.org/10.26866/jees.2022.6.r.134.

[8] M. Boumalkha, et al., Design of highly efficient filtering power amplifier with a wideband response for sub-6 GHz 5G applications, Results. Eng. 24 (Dec. 2024), https://doi.org/10.1016/j.rineng.2024.102905.

[9] J. Liu, Y.X. Wang, G.Y. Wei, R.L. Jia, Y.L. Duan, Design of high-selective wideband bandpass filter with a notched-band and harmonic suppression, Prog. Electromagnet. Res. Lett. 105 (2022) 57–62, https://doi.org/10.2528/PIERL22051001, no. July.

[10] D. Saha, I. Mohd Nawi, and M. Zakariya, "Journal pre-proof super low profile 5G mmWave highly isolated MIMO antenna with 360 • pattern diversity for smart city IoT and vehicular communication super low profile 5G mmWave highly isolated MIMO antenna with 360 • pattern diversity for smart city IoT and vehicular communication," 2024, doi: 10.1016/j.rineng.2024.103209.

[11] Y.P. Lim, Y.L. Toh, S. Cheab, G.S. Ng, P.W. Wong, Chained-Function Waveguide Filter for 5G and beyond, in: IEEE Region 10 Annual International Conference, Proceedings/TENCON, 2019, pp. 107–110, https://doi.org/10.1109/TENCON.2018.8650548, 2018-Octob, no. October.

[12] Y. Sung, A novel dual-mode dual-band bandpass filter based on a single ring resonator, J. Electromagnet. Eng. Sci. 20 (2) (2020) 91–95, https://doi.org/10.26866/JEES.2020.20.2.91.

[13] Y.P. Lim, S. Cheab, S. Soeung, P.W. Wong, On the design and fabrication of chained-function waveguide filters with reduced fabrication sensitivity using CNC and DMLS, Progr. Electromagnet. Res. B 87 (2020) 39–60, https://doi.org/10.2528/PIERB20011101, no. January.

[14] A.O. Nwajana, E.R. Obi, Application of Compact Folded-Arms Square Open-Loop Resonator to Bandpass Filter Design, Micromachines 14 (2) (Feb. 2023), https://doi.org/10.3390/mi14020320.

[15] C. E. C. S. Lucyszyn, "Seed function combination selection for chained function filters," no. July 2010, 2014, 10.1049/iet-map.2009.0508.

[16] H.S. Im, S.W. Yun, Design of a dual-band bandpass filter using an open-loop resonator, J. Electromagnet. Eng. Sci. 17 (4) (2017) 197–201, https://doi.org/10.26866/jees.2017.17.4.197.

[17] L. Zhu, R. Payapulli, S.-H. Shin, M. Stanley, N.M. Ridler, S. Lucyszyn, 3-D Printing Quantization Predistortion Applied to Sub-THz Chained-Function Filters, IEEe Access. 10 (2022), https://doi.org/10.1109/access.2022.3162586, 1–1.

[18] D.C.H. Bong, V. Jeoti, S. Cheab, P.W. Wong, Design and Synthesis of Chained-Response Multiband Filters, IEEe Access. 7 (2019) 130922–130936, https://doi.org/10.1109/access.2019.2940059.

[19] Y.P. Lim, S. Cheab, S. Soeung, P.W. Wong, On the design and fabrication of chained-function waveguide filters with reduced fabrication sensitivity using CNC and DMLS, Progr. Electromagnet. Res. B 87 (2020) 39–60, https://doi.org/10.2528/PIERB20011101, no. January.

[20] C.Y. Chuan, C. Sovuthy, Design and Synthesis of Parallel Connected Chained Function Filter, in: *APACE 2019 - 2019 IEEE Asia-Pacific Conference on Applied Electromagnetics, Proceedings*, no. November, 2019, pp. 25–27, https://doi.org/10.1109/APACE47377.2019.9020899.

[21] U. Patel, et al., Split ring resonator geometry inspired crossed flower shaped fractal antenna for satellite and 5G communication applications, Results. Eng. 22 (Jun. 2024), https://doi.org/10.1016/j.rineng.2024.102110.

[22] M.S. Castanho, C.K. Dominicini, M. Martinello, M.A.M. Vieira, Chaining-Box: A Transparent Service Function Chaining Architecture Leveraging BPF, IEEE Trans. Network Serv. Manage. 19 (1) (Mar. 2022) 497–509, https://doi.org/10.1109/TNSM.2021.3122135.

[23] S. Cheab, P.W. Wong, X.Y. Chew, Parallel Connected Dual-Mode Filter, IEEE Microwave Wirel. Components Lett. 25 (9) (2015) 582–584, https://doi.org/10.1109/LMWC.2015.2451393.

[24] G.S. Ng, S. Cheab, P.W. Wong, S. Soeung, Synthesis of chained-elliptic function waveguide bandpass filter with high rejection, Progr. Electromagnet. Res. C 99 (2020) 61–75, https://doi.org/10.2528/pierc19112002, no. November 2019.

[25] A.M. Soreng, A. Mishra, Design techniques of microwave cavity and waveguide filters: a literature review, Int. J. Eng. Tech. Res. 8 (4) (2018) 55–61.

[26] Z. Zhang, et al., Microwave Displacement Sensors Based on Filtering Phase Shifter with Chebyshev Response, IEEE Sens. J. 24 (10) (May 2024) 15857–15864, https://doi.org/10.1109/JSEN.2024.3379754.

[27] R. Gómez-garcía, S. Member, L. Yang, and D. Psychogiou, "Single /Multi-Band Coupled-Multi-Line Filtering Section and Its Application to RF Diplexers, Bandpass / Bandstop Filters, and Filtering Couplers," vol. 67, no. 10, pp. 3959–3972, 2019.

[28] X. Li, Y. Wang, W. Xu, A New Filtering Scheme for HVDC Terminals Based on Damped High-Pass Filter, IEEE Trans. Power Deliv. 34 (5) (2019) 2050–2057, https://doi.org/10.1109/TPWRD.2019.2895084.

[29] P.W. Wong, A Sustainable and Fast Approach to Filter Design for 5G Implementation, in: RFM 2018 - 2018 IEEE International RF and Microwave Conference, Proceedings 88, 2018, pp. 349–351, https://doi.org/10.1109/RFM.2018.8846520.

[30] S. Cheab, P.W. Wong, S. Soeung, Design of multi-band filters using parallel connected topology, Radioengineering 27 (1) (2018) 186–192, https://doi.org/10.13164/re.2018.0186.

[31] W.S. Chang, C.Y. Chang, Analytical design of microstrip short-circuit terminated stepped-impedance resonator dual-band filters, IEEE Trans. Microw. Theory. Tech. 59 (7) (2011) 1730–1739, https://doi.org/10.1109/TMTT.2011.2132140.

[32] N. Khajavi, S.V.A.D. Makki, S. Majidifar, Design of high-performance microstrip dual-band bandpass filter, Radioengineering 24 (1) (2015) 32–37, https://doi.org/10.13164/re.2015.0032.

[33] P. Ma, et al., A Design Method of Multimode Multiband Bandpass Filters, IEEe Trans. Microw. Theory. Tech. 66 (6) (2018) 2791–2799, https://doi.org/10.1109/TMTT.2018.2815682.

[34] F. De Paolis, "Satellite Filters for 5G/6G and beyond," in *2021 IEEE MTT-S International Microwave Filter Workshop, IMFW 2021*, Institute of Electrical and Electronics Engineers Inc., 2021, pp. 148–150. 10.1109/IMFW49589.2021.9642277.

[35] I.C. Hunter, L. Billonet, B. Jarry, P. Guillon, Microwave filters - Applications and technology, IEEe Trans. Microw. Theory. Tech. 50 (3) (2002) 794–805, https://doi.org/10.1109/22.989963.

[36] I. C. Hunter, *Theory and Design of Microwave Filters*.

[37] M. Šašić, S.T. Imeci, Design of microstrip coupledline bandpass filter, Heritage Sustainable Dev. 3 (1) (2021) 44–52, https://doi.org/10.37868/hsd.v3i1.55.

[38] A.I. Abunjaileh, I.C. Hunter, Direct synthesis of parallel-connected symmetrical two-port filters, IEEE Trans. Circuits Syst. II: Express Briefs 57 (12) (2010) 971–974, https://doi.org/10.1109/TCSII.2010.2083190.

[39] M. Meng, I.C. Hunter, J.D. Rhodes, The design of parallel-connected filter networks with nonuniform Q resonators, IEEE Trans. Microw. Theory. Tech. 61 (1) (2013) 372–381, https://doi.org/10.1109/TMTT.2012.2230021.

[40] T. Huang, H. Liu, C. Guo, L. Feng, L. Geng, 3-D Printed mm-Wave Filter Using Increased-Height DGS Resonator for Spurious Suppression, IEEE Trans. Circuits Syst. II: Express Briefs 69 (11) (2022) 4293–4297, https://doi.org/10.1109/TCSII.2022.3187970.

[41] V.B. Narayane, G. Kumar, A Selective Wideband Bandpass Filter With Wide Stopband Using Mixed Lumped-Distributed Circuits, IEEE Trans. Circuits Syst. II: Express Briefs 69 (9) (2022) 3764–3768, https://doi.org/10.1109/TCSII.2022.3173472.

[42] T.K. Das, S. Chatterjee, S.K.A. Rahim, T.K. Geok, Compact High-Selectivity Wide Stopband Microstrip Cross-Coupled Bandpass Filter with Spurline, IEEE Access. 10 (2022) 69866–69882, https://doi.org/10.1109/ACCESS.2022.3187408, no. July.

[43] G. Lin, S. Member, Y. Dong, and S. Member, "A Compact, Hybrid SIW Filter With Controllable Transmission Zeros and High Selectivity," vol. 69, no. 4, pp. 2051–2055, 2022.

[44] L. Qi, D. Xing, R. Wang, X. Qi, J. Zhao, Coupling matrix synthesis of general Chebyshev filters, MATEC Web Conf. 309 (2020) 01011, https://doi.org/10.1051/matecconf/202030901011.
[45] C. H. Mahadevaswamy, A. R. Vasistha, A. O. Nwajana, C. H. Mahadevaswamy, A. R. Vasistha, and A. O. Nwajana, "Dual-band bandpass filter derived from the transformation of a single-band bandpass filter." [Online]. Available: https://www.researchgate.net/publication/381728755.
[46] Y. Leong, S. Cheab, S. Soeung, P.W. Wong, A new class of dual-band waveguide filters based on chebyshev polynomials of the second kind, IEEE Access. 8 (2020) 28571–28583, https://doi.org/10.1109/ACCESS.2020.2972160.
[47] A. Bingler, S. Bilicz, M. Csornyei, Global sensitivity analysis using a kriging metamodel for em design problems with functional outputs, IEEE Trans. Magn. 58 (9) (Sep. 2022), https://doi.org/10.1109/TMAG.2022.3167105.
[48] V. Lesnikov, T. Naumovich, A. Chastikov, Sensitivity analysis of digital filters using the continued fraction expansion, in: Moscow Workshop on Electronic and Networking Technologies, MWENT 2018 - Proceedings, 2018, pp. 1–5, https://doi.org/10.1109/MWENT.2018.8337178, vol. 2018-March.
[49] S. Saleh, M.H. Jamaluddin, F. Razzaz, S.M. Saeed, Compact 5G Nonuniform Transmission Line Interdigital Bandpass Filter for 5G/UWB Reconfigurable Antenna, Micromachines 13 (2022), https://doi.org/10.3390/mi13112013, 2013.
[50] Sahar Saleh, Widad Ismail, Intan S.Zainal Abidin, Moh'd H. Jamaluddin, Compact 5G Hairpin Bandpass Filter Using Non-Uniform Transmission Lines Theory, ACES J. 36 (2) (Feb. 2021) 126–131.